Hindawi
Advances in Materials Science and Engineering
Volume 2023, Article ID 9793538, 1 page
https://doi.org/10.1155/2023/9793538

Retraction

Retracted: Antidandruff Activity of Polyherbal (*Murraya koenigii*, *Moringa oleifera*, and *Psidium guajava*) Extract against *Malassezia* Species: In Silico Studies

Advances in Materials Science and Engineering

Received 26 December 2023; Accepted 26 December 2023; Published 29 December 2023

Copyright © 2023 Advances in Materials Science and Engineering. This is an open access article distributed under the Creative Commons Attribution License, which permits unrestricted use, distribution, and reproduction in any medium, provided the original work is properly cited.

This article has been retracted by Hindawi, as publisher, following an investigation undertaken by the publisher [1]. This investigation has uncovered evidence of systematic manipulation of the publication and peer-review process. We cannot, therefore, vouch for the reliability or integrity of this article.

Please note that this notice is intended solely to alert readers that the peer-review process of this article has been compromised.

Wiley and Hindawi regret that the usual quality checks did not identify these issues before publication and have since put additional measures in place to safeguard research integrity.

We wish to credit our Research Integrity and Research Publishing teams and anonymous and named external researchers and research integrity experts for contributing to this investigation.

The corresponding author, as the representative of all authors, has been given the opportunity to register their agreement or disagreement to this retraction. We have kept a record of any response received.

References

[1] A. Sharma, P. Sakthiselvan, V. Karthick et al., "Antidandruff Activity of Polyherbal (*Murraya koenigii*, *Moringa oleifera*, and *Psidium guajava*) Extract against *Malassezia* Species: In Silico Studies," *Advances in Materials Science and Engineering*, vol. 2022, Article ID 7373942, 13 pages, 2022.

Hindawi
Advances in Materials Science and Engineering
Volume 2022, Article ID 7373942, 13 pages
https://doi.org/10.1155/2022/7373942

RETRACTED

Research Article

Antidandruff Activity of Polyherbal (*Murraya koenigii*, *Moringa oleifera*, and *Psidium guajava*) Extract against *Malassezia* Species: In Silico Studies

Akshata Sharma,[1] **Punniavan Sakthiselvan**,[1] **V. Karthick**,[2] **R. Subraja**,[3] **T. Srinivasan**,[4] **K. Amudha**,[5] **and Shani T John**[6]

[1]*Department of Bio-Engineering, Vels Institute of Science Technology and Advanced Studies (VISTAS), Chennai 600117, India*
[2]*Centre for Ocean Research (DST-FIST Sponsored Centre), MoES-Earth Science & Technology Cell (ESTC), Sathyabama Institute of Science and Technology, Jeppiaar Nagar Rajiv Gandhi Salai, Chennai 600119, India*
[3]*Department of Biotechnology, Sathyabama Institute of Science and Technology, Jeppiaar Nagar Rajiv Gandhi Salai, Chennai 600119, India*
[4]*Centre for Research and Development, Department of Microbiology, Hindustan College of Arts & Science, Chennai, Tamil Nadu, India*
[5]*Department of Biochemistry, Sri Sankara Arts and Science College (Autonomous), Enathur, Kanchipuram, Tamil Nadu, India*
[6]*Department of Biology, School of Natural Science, Madawalabu University, Post Box No. 247, Bale Zone, Robe, Oromiya Region, Ethiopia*

Correspondence should be addressed to Punniavan Sakthiselvan; psakthiselvan.se@velsuniv.ac.in and Shani T John; shani.dip@gmail.com

Received 27 January 2022; Accepted 22 April 2022; Published 26 May 2022

Academic Editor: Palanivel Velmurugan

Copyright © 2022 Akshata Sharma et al. This is an open access article distributed under the Creative Commons Attribution License, which permits unrestricted use, distribution, and reproduction in any medium, provided the original work is properly cited.

Dandruff is one of the leading causes of hair fall and is commonly caused by bacterial and fungal species especially the *Malassezia* species. The lipolytic enzymes of the *Malassezia* species play an important role in obtaining lipids from the environment, and they are necessary for the growth and pathogenicity of *Malassezia*. Therefore, the lipases of the three most commonly (*Malassezia globosa*, *Malassezia furfur,* and *Malassezia restricta)* affecting *Malassezia* species have been taken for the *In-silico* studies. The three-dimensional structure of the lipase of *Malassezia globosa* (PDB ID: 4ZRE) was retrieved from protein data bank, and the other two proteins of the two species (*Malassezia furfur* and *Malassezia restricta*) were built using homology modelling by Swiss modeler. The lipases of the *Malassezia* species along with the 16 bioactive compounds of the polyherbal (*Murraya koenigii, Moringa oleifera,* and *Psidium guajava*) ethanolic extract predicted by GC-MS analysis were taken for the molecular docking studies. The pharmacokinetic properties of the bioactive compounds were predicted. Thus, the molecular docking results revealed that the bioactive compound flavone with score of −7.160 Kcal/mol, isopropyl stearate with binding score of −10.107 Kcal/mol, and eugenol with a binding score of −8.296 Kcal/mol have shown good binding affinity against the lipase of *Malassezia restricta, Malassezia globosa,* and *Malassezia furfur,* respectively. Hence, these compounds can be further investigated by *in-vitro* and *in-vivo* studies to be used as potential drug candidates.

1. Introduction

The swiftly developing world has occupied the people with scheduled works and commitments where the people have forgotten to take care of themselves. It is such a handcuffed situation that people find very few hours for taking care of themselves. The dandruff is one such skin disease caused due to improper hair care. The dandruff is a common skin condition that causes flaking on the scalp. Generally, dandruff is caused by the bacterial species such as *Staphylococcus aureus, Propionibacterium,* and fungal species like *Candida* and *Malassezia species*. The causes of dandruff are generally

unknown but leaving the scalp dry may be one of the reasons for dandruff. Furthermore, during the winter season, the condition may even get worse [1]. The *Malassezia* species are the most common form of yeast that causes dandruff. The lipolytic enzymes of the *Malassezia* species are responsible for the growth and pathogenicity of the species. The lipase protein of the *Malassezia* species metabolizes the triglycerides of the sebum present in the skin and releases a lipid by-product called oleic acid which is a free fatty acid. Oleic acid penetrates the top layer of the *epidermis*, the stratum corneum, and evokes an inflammatory response in susceptible people which disturbs homeostasis and results in erratic cleavage of stratum corneum cells. During the dandruff, the *Malassezia* species increases by 2 times by metabolizing many lipid molecules [2–4]. The phospholipases of the *Malassezia* species hydrolyze the glycerophospholipids present in the skin. Moreover, the lipases and phospholipases are also present in the bacteria such as *Propionibacterium* and *Staphylococcus aureus* and some fungi, for example, *Aspergillus fumigatus*, *Candida albicans*, and *Cryptococcus neoformans,* where it plays a pivotal role in the occurrence of skin lesions [5–7]. Several allopathic medicines are available in the market to control the dandruff which is given in the form of antifungal creams and shampoos containing ketoconazole or salicylic acid. The side effects of ketoconazole include nausea, headache, breast swelling, dizziness, stomach pain, and diarrhea. Thus, people prefer herbal medicines which are more convenient as they have very low detrimental effects; thus, they are being used to treat dandruff. Some of the herbs used in the treatment are amla, bhringaraj, hibiscus, neem, ginger, coconut, and tulasi. Additionally, the other herbs, which can reduce the dandruff, are curry leaves, moringa leaves, and guava leaves. Each of them has their own ability to cure dandruff. The present study is done to enhance the antidandruff property for better results. The curry leaves are scientifically known as *Murraya koenigii*, a subtropical plant native to Asia. *Murraya koenigii* belongs to the family of Rutaceae, and in India it is distributed over the regions of Himalayas, Uttarakhand, Assam, West Bengal, Western Ghats, Travancore, and cochin. Recently, the commercial plantation of *Murraya koenigii* is also done in Australia, Nepal, Malaysia, Pakistan, Sri Lanka, Thailand, Vietnam, Bhutan, and so on. *Murraya koenigii* generally grows best in well-drained soil in areas with full sun light or partial shade. The fresh leaves are used as seasoning in many dishes in the southern and southeast Asia [8–10]. *M. koenigii* is well known for its medicinal properties, which includes antibacterial, antifungal, antidiabetic, antitumor, anticancer, antiulcer, antidiarrheal, antihelminthic, antiamnesic, radioprotective, chemoprotective, antilipid peroxidative, wound healing, memory enhancing, antitumor, vasodilating effect, phagocytic activity, anti-hair-fall, and skin pigmentation properties [11, 12]. The drumstick tree leaves are scientifically known as *Moringa oleifera,* which are native to Indian subcontinent. The *Moringa oleifera* is a fast -growing plant and belongs to the family of Moringaceae [13]. The young sea pods and leaves are being used as vegetables and traditional medicine in Indian ayurvedic medical systems. The medicinal properties of *Moringa oleifera* include antitumor, antipyretic, antiepileptic, anti-inflammatory, antiulcer, antispasmodic, diuretic, antihypertensive, cholesterol lowering, antioxidant, antidiabetic, hepatoprotective, antibacterial, and antifungal activities. The *Moringa oleifera* is distributed over the central America and the Caribbean, northern countries of South America, Africa, and south and southeast Asia [14]. The Guava tree scientifically known as *Psidium guajava* is a small tree belonging to the family of Myrtaceae. Psidium guajava is native to Mexico, Central America, the Caribbean, and the Northern South America. The medicinal properties of *Psidium guajava* include antidiabetic, anti-bacterial, antifungal, antidiarrheal, anti-cancer, wound healing, gastrointestinal problem, antioxidant, and anti-dandruff properties. Major guava producing states in India are Bihar, Uttar Pradesh, Maharashtra, Karnataka, Orissa, West Bengal, Andhra Pradesh, and Tamil Nadu [15]. Therefore, the polyherbal (*Murraya koenigii, Moringa oleifera,* and *Psidium guajava*) ethanolic extract identified with 16 bioactive compounds, and the lipases of three most common species of *Malassezia,* which are *Malassezia globosa, Malassezia furfur,* and *Malassezia restricta* have been taken for the In-silico studies. The three-dimensional structure of lipase of *Malassezia globosa* was studies and retrieved from protein data bank with PDB ID: 4ZRE. While the 3D structure of other two lipases was constructed with the help of homology modelling. They were further taken for the molecular docking studies to find out the efficacy of the ligand molecule, which can be developed into a drug in the future.

2. Materials and Methods

2.1. Homology Modelling of Lipase Protein from Malassezia Species. The present study involves wide use of software, which includes AutoDock 4.2.6, MGL Tools 1.5.4, Python 3.8.2, Discovery Studio visualizer 3.1, PyMOL 2.3, and SwissPDB viewer. Apart from these, there are several web servers involved, which includes SWISS-MODEL (https://swissmodel.expasy.org/) for homology modelling of proteins with unknown three-dimensional structure [16]. PROCHECK and ERRAT (https://servicesn.mbi.ucla.edu/SAVES/) are used to generate Ramachandran plot and frequencies of noncovalent structural bonding elucidation between many atoms in the protein [17]. Clustal Omega (https://www.ebi.ac.uk/Tools/msa/clustalo/) is for multiple sequence alignment. Blast-P (https://blast.ncbi.nlm.nih.gov/Blast.cgi?PAGE=Proteins) is for sequence similarity based on the protein data bank [18]. The 3-dimensional structures of the lipase of *Malassezia furfur* and *Malassezia restricta* were not available in the protein data bank. Hence, the protein was modelled using homology modelling using the SWISS-MODEL software. The sequence similarity between the query sequences was done using the BLAST-P web server, where the amino acid FASTA sequence was retrieved from the UniProtKB database, and the structural homologs were searched in the BLAST-P against the Protein data bank database to find the closely related structure with respect to the query sequence and similarity

RETRACTED

[19]. Multiple sequence alignment of the protein FASTA sequence was done using the Clustal Omega web server to analyze the conserved regions [20]. SWISS-MODEL is an authentic web server developed by the Swiss Institute of Bioinformatics, which is a widely used automated server for homology modelling of proteins to predict the 3-dimensional structure of proteins as the 3-dimensional structure of proteins is essential since it provides insights to its structure, properties, mutagenesis, and functions [21]. Hence, the development of drug can be done with the help of these 3-dimensional structures, properties, and function. The FASTA sequence of the target sequence was fed into the web server along with the template taken from the results of BLAST-P, and the template structure was fed for each of the protein for modelling. Totally, 10 models were built using Swiss model and the lowest energy model conformation was chosen as the best. The best model generated by either of the models was further subjected to energy minimization using the SwissPDB viewer. Furthermore, the validation of the model was done with the help of saves webserver (https://saves.mbi.ucla.edu/).

2.2. Molecular Docking Studies of Lipases of the Malassezia Species

2.2.1. Determination of Phytocomponents of the Polyherbal Ethanolic Extract by Gas-Chromatography-Mass Spectrometry Analysis. Totally, 16 phytocomponents were revealed using GC-MS analysis by injecting the polyherbal ethanolic extract into an HP−5 column (30 m × 0.25 mm i.d with 0.25 μm film thickness), Agilent technologies 6890 N JEOL GC Mate II GC-MS model. The following chromatographic conditions were used: helium was the carrier gas, the flow rate was 1 mL/min; and the injector was operated at 200°C, and column oven temperature was programmed as 50–250°C at a rate of 10°C/min injection mode. The following MS conditions were used: ionization voltage was 70 eV; ion source temperature was 250°C; interface temperature was 250°C; and the mass range was 50–600 mass units [22]. The database of the National Institute of Standard and Technology (NIST) was used for the interpretation of the mass spectrum of GC-MS. These 16 phytocomponents were taken for the molecular docking studies.

2.2.2. Screening of Protein Ligand Library. The 16 phytocomponents were screened using Lipinski rule of five, which involves five parameters they are molecular weight (<500 KDa), hydrogen bond donor (<5), hydrogen bond acceptor (<10), lipophilicity Log P (<5), and molecular refractivity (40–130). Additionally, the phytocompounds displaying R05 violations were removed. Therefore, only 11 components satisfied the Lipinski rule and were taken for the In-silico studies. The lipase protein for the *Malassezia globosa* was studied and retrieved from protein data bank (PDB ID: 4ZRE) which is maintained by National Centre for Biotechnology Information (NCBI). The modelled lipase for *Malassezia furfur* and *Malassezia restricta* was also taken for the molecular docking studies. A single chain was determined for the docking analysis where the heteroatomic molecules, hydrophobic molecules were removed, and further conformations was visualized using PyMOL viewer. The protein binding site was predicted for each protein by using CastP web server (http://sts.bioe.uic.edu/castp/index.html?3trg) [23].

2.2.3. Virtual Ligand Screening. The molecular docking was performed using Autodock 4.2 software. This software recognizes the binding efficiency of the ligand which is docked against the protein lipase of the *Malassezia* species. This software is made to understand the protein-protein interaction or protein-ligand interaction which is based on the Lamarckian genetic algorithm. The Autodock 4.2 is a two-step process, where the grid parameters are set by addition of hydrogen bonds and charges. The grid parameters were set at dimensions X:64 Å; Y:68 Å; and Z:50 Å, with grid points for the total map being 228735. The centre grid box size was set with *X* axis:−6.250 Å, *Y* axis: 2.222 Å, and *Z*-axis:−8.556 Å, for lipase of *Malassezia globosa* (PDB ID: 4ZRE). For lipase of *Malassezia restricta*, the grid parameters were set at dimensions *X*: 40 Å, *Y*:40 Å, and *Z*:40 Å, with grid points for the total map being 64000, and the centre grid box size was set with *X* axis:−10.778 Å, *Y* axis:−2.333 Å, and *Z* axis: 4.667 Å. For the lipase protein of *Malassezia furfur*, the grid parameters were set at dimensions *X*: 40 Å, *Y*: 40 Å, and *Z*: 40 Å, with grid points for the total map being 64000. The default grid spacing was set the same for all the proteins, that is, 0.375 Å. The interaction of the protein with their ligand forms the basis of the drug development process. The binding energy is obtained for each ligand and the protein ligand complex was analyzed using discovery studios 3.1 [24].

2.2.4. Visualization of Docking Conformation by Discovery Studios 3.1. The Discovery studio 3.1 is a software which is used to visualize the 2D and 3D conformations of the protein-ligand complex. This software helps to view the interactions such as van der Waals interaction and conventional hydrogen bonding. It also helps in visualizing the surface images, which shows the conformation of structure-based ligand protein docking against the targeted proteins (lipase). Discovery studios 3.1 software is maintained by Dassault system [25].

2.2.5. Screening of Drug Properties. The ADMET are the drug likeness properties of the ligand. It is an analysis of the ligand to evaluate the absorption, distribution, metabolism, excretion, and toxicity level of the drug. The major parameters to be noted are solubility, gastrointestinal absorption, penetration of the drug in the blood-brain barrier and central nervous system, and the toxicity level in the humans and rats. These properties are based on the principle of vector-based algorithm which can easily dataset known inhibitor/non-inhibitor as well as substrate/non-substrate. These parameters were analyzed using SwissADME webserver (http://www.swissadme.ch/), which helps in calculating the behavior and characteristics of drug compounds [26].

RETRACTED

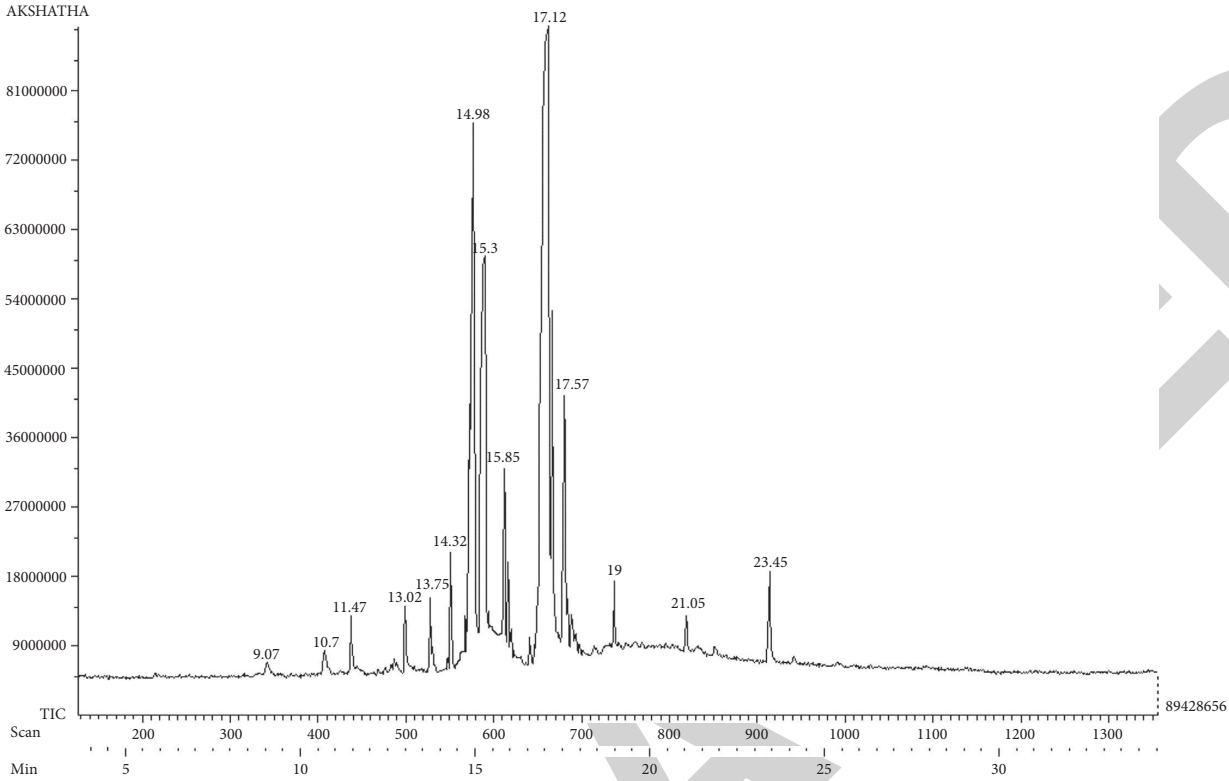

Figure 1: Gas chromatogram of polyherbal ethanolic extract indicating bioactive compounds.

Table 1: Phytocomponents of polyherbal ethanolic extracts identified by GC-MS analysis.

S.No.	Compound name	Molecular formula	Molecular weight	Retention time (min)	Peak area (%)
1.	A-pinene	$C_{10}H_{16}$	136.23	9.07	1.23
2.	4-hydroxy-3-methoxy benzyl alcohol	$C_8H_{10}O_3$	154.16	10.7	2.25
3.	Eugenol	$C_{10}H_{12}O_2$	164.20	11.47	1.12
4.	A-caryophyllene	$C_{15}H_{24}$	204.35	13.75	2.46
5.	Humulene-v1	$C_{15}H_{24}$	204.35	14.32	3.58
6.	Flavone	$C_{15}H_{10}O_2$	222.24	14.98	19.15
7.	n-hexadecanoic acid	$C_{16}H_{32}O_2$	256.42	15.3	9.92
8.	Tetra decanoic acid, propyl ester	$C_{17}H_{34}O_2$	270.45	15.85	2.12
9.	Hexadecanoic acid, ethyl ester	$C_{18}H_{36}O_2$	284.48	15.85	2.12
10.	8-octadecenoic acid, methyl ester	$C_{18}H_{34}O_2$	282.46	17.12	45.05
11.	(Z)-13-Octadecen1-yl acetate	$C_{20}H_{38}O_2$	310.51	17.57	6.94
12.	Phenol,2,4-Bis[1,1–dimethylethyl]	$C_{17}H_{30}OSi$	278.50	12.77	2.69
13.	Docosanoic acid, methyl ester	$C_{23}H_{46}O_2$	354.61	21.05	1.12
14.	Trans-A-copaene	$C_{15}H_{24}$	204.35	13.02	2.68
15.	Isopropyl stearate	$C_{21}H_{42}O_2$	326.56	19	1.08
16.	2,6-Bis[3-nitrobenzylidine]-4-methylcyclohexanone	$C_{20}H_{16}N_2O_5$	364.35	23.45	0.89

3. Results and Discussion

3.1. Gas-Chromatography and Mass Spectrometry Analysis. The GC-MS chromatogram of polyherbal ethanolic extract indicated 16 peaks that were recognized by relating their peak retention time, peak area (%), height (%), and mass spectral fragmentation patterns to those of the known compounds described by the National Institute of Standards and Technology (NIST) library (Figure 1). The bioactive compounds of polyherbal ethanolic extract revealed by gas chromatography and mass spectrometry analysis are given in Table 1 along with the retention time and peak area. The bioactive compounds such as A-pinene (1.23%), 4-hydroxy-3-methoxy benzyl alcohol (2.55%), eugenol (1.12%), A-caryophyllene (2.46%), Trans-A-copaene (2.68%), humulene-v1(3.58%), Flavone (19.15%), n-hexadecanoic acid (9.92%), tetradecanoic acid, propyl ester (2.12%), hexadecanoic acid, ethyl ester (2.12%), 8-octadecenoic acid, methyl ester(45.05%), (Z)-13-octadecen1-yl acetate (6.94%), isopropyl stearate (1.08%), docosanoic acid, methyl ester

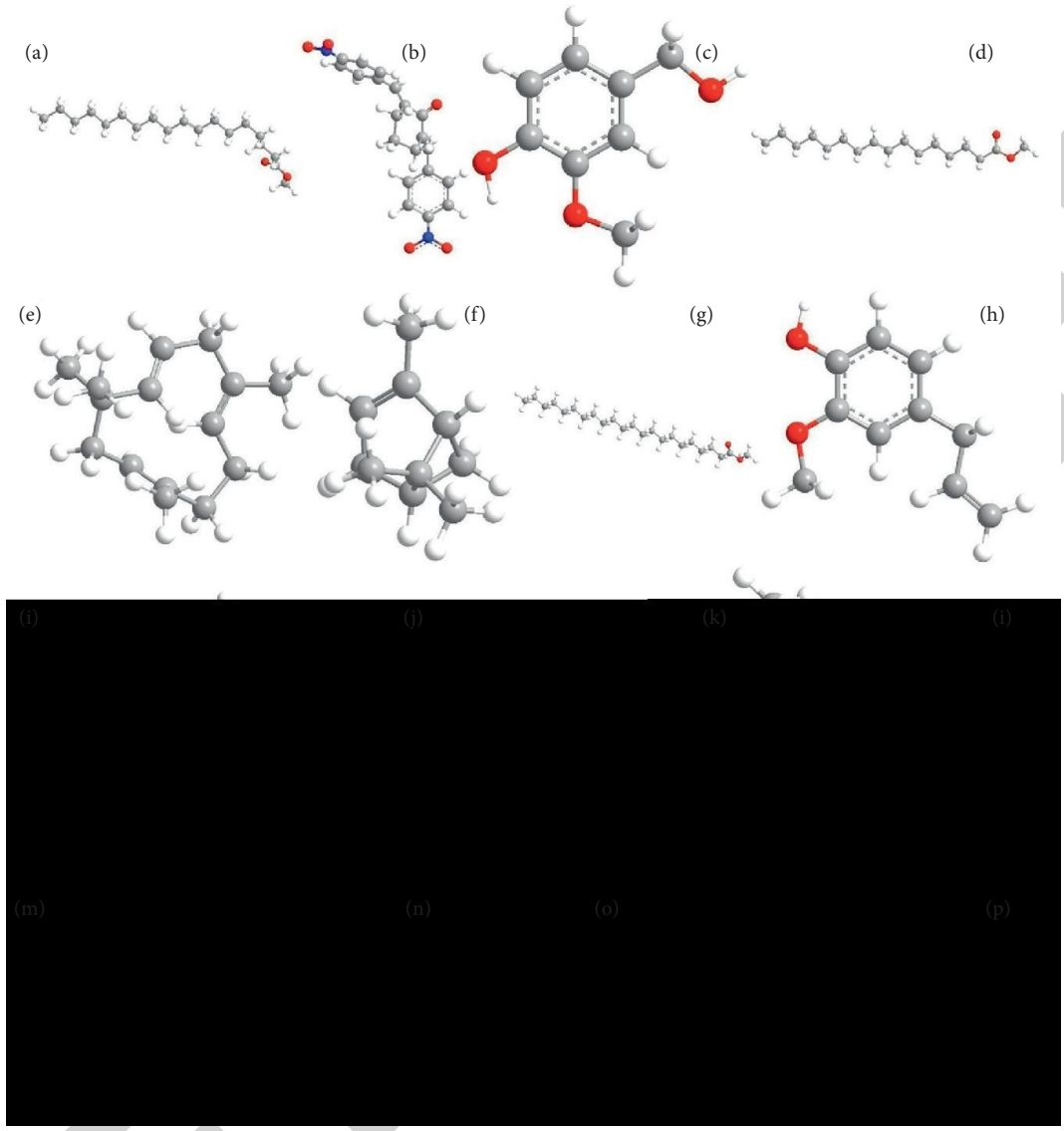

Figure 2: Bioactive compounds of polyherbal ethanolic extract (a) (Z)-13-Octadecen1-yl acetate, (b)2,6-Bis[3-nitrobenzylidine]-4-methylcyclohexanone, (c) 4-hydroxy-3-methoxy benzyl alcohol, (d) 8-octadecenoic acid, methyl ester, (e) A-caryophyllene, (f) A-pinene, (g)docosanoic acid, methyl ester, (h)eugenol, (i)flavone, (j)hexadecanoic acid, ethyl ester, (k)humulene-v1,(l) isopropyl stearate, (m) phenol,2,4-Bis[1,1-dimethylethyl], (n)n-hexadecanoic acid, (o)Trans-A-copaene, and (p) tetra decanoic acid, propyl ester.

(1.12%), 2,6-Bis[3-nitrobenzylidine]-4-methylcyclohexanone (0.89%), and phenol,2,4-Bis[1,1-dimethylethyl] (2.69%) were identified via GC-MS analysis (Figure 2). The 8-octadecanoic acid, methyl ester is a fatty acid which has antioxidant, anti-inflammatory, and antimicrobial activity. Eugenol, a-caryophyllene, flavone, and n-hexadecanoic acid are well known for its antioxidant, anti-inflammatory, and antimicrobial activity, and these compounds were elucidated and recorded [23]. Also, eugenol has been claimed to have antiseptic activities and antineoplastic activity [24].

3.2. Homology Modelling of Lipase Protein of Malassezia Species Using SWISS-MODEL. BLAST-P structural and sequential similarity was found identified. For the lipase of *Malassezia restricta,* the monoacylglycerol and diacylglycerol lipase protein of *Malassezia globosa* with PDB ID: 3UUE with 1.45 Å resolution showed the sequence similarity of 74% followed by lipase protein of *Malassezia globosa* of PDB ID: 4ZRD with 2.3 Å, which showed the sequence similarity of 73%; thus, the protein with PDB ID 3UUE was chosen as template and proceeded to build model. For the lipase of *Malassezia furfur,* the lipase protein of *Candida Antarctica* of PDB ID: 2VEO with 2.2 Å resolution showed the sequence similarity of 35% followed by lipase protein of the *Candida Antarctica* with 2.1 Å, and the lipase protein with PDB ID: 2VEO was chosen as template and proceeded to build model. Validating the built model is a very essential step that denotes the built model quality and reliability. Ramachandran plot is used to validate the model whether or not any amino acids are present in the disallowed regions due to steric hindrance of phi (φ) and psi (ψ) bonds between C-alpha methylene group

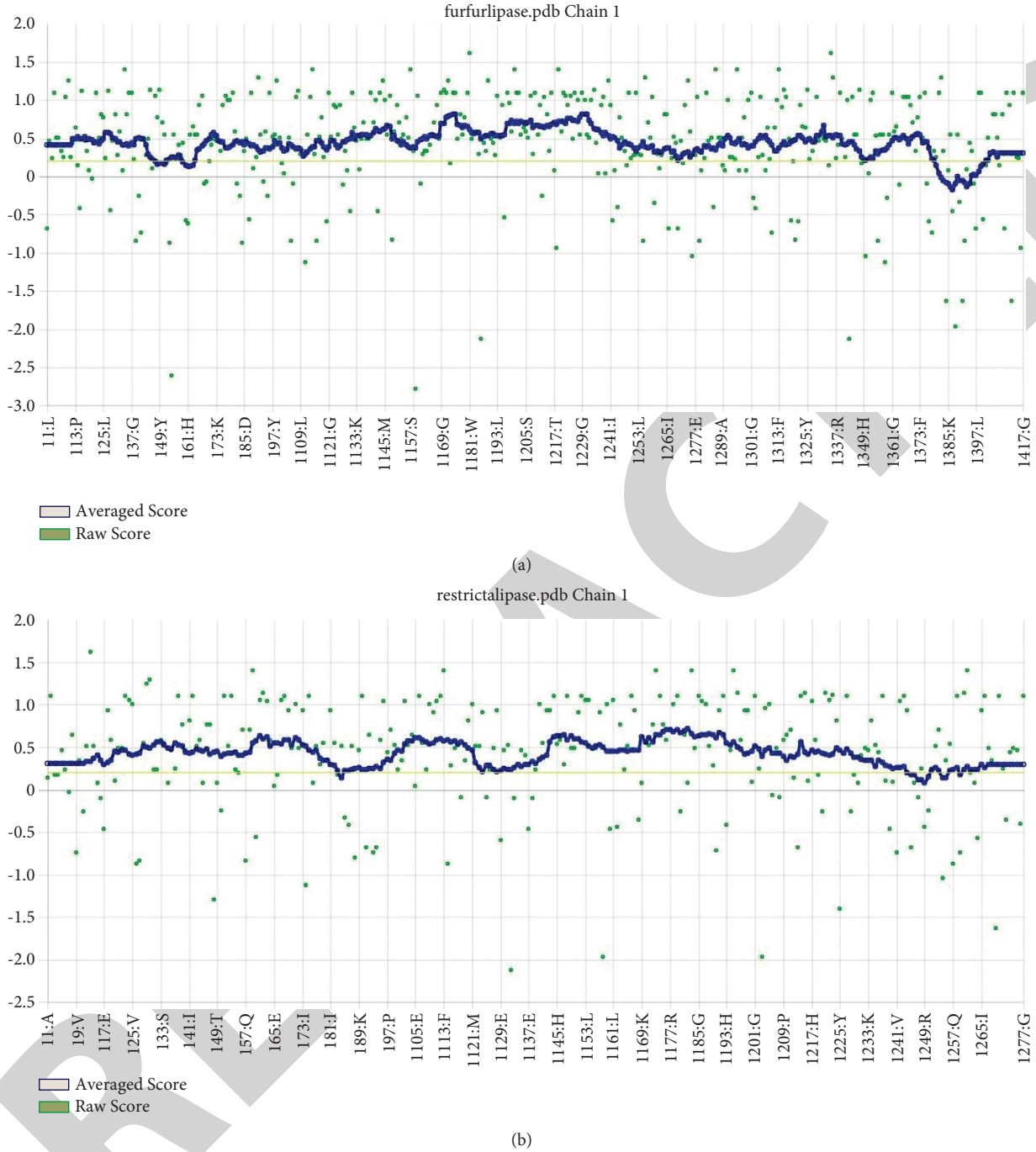

Figure 3: Verify 3D plot for Lipase of (a) *Malassezia furfur* and (b) *Malassezia restricta*.

side chain and main chain atoms in a polypeptide [27]. The PDB file format of models built using SWISS-MODEL was submitted to the PROCHECK web server to check for the same (Figure 3). Ramachandran plots were analyzed and the observations were studied and reported (Figure 4). The model of furfur lipase developed by SWISS-MODEL showed the best results with 85.1% (303 amino acids) of amino acids in the most favored regions of the plot; 13.8% (49 amino acids) in additional allowed regions; 0.3% (1 amino acid) in generously allowed regions; and 0.8% (3 amino acids SER201, THR 417, and ALA 429) in the disallowed region(s) out 417 amino acid residues. The overall G-value for modelled protein furfur lipase was found to be −0.01, which shows that modelled protein is acceptable; a G-value lower than −0.5 is considered unusual. The model of restricta lipase developed by SWISS-MODEL showed the best results with 91.3% (211 amino acids) of amino acids in the most favored regions of the plot; 6.5% (15 amino acids) in additional allowed regions; 1.7% (4 amino acid) in generously allowed regions; and 0.4% (1 amino acid ASN 245) in the disallowed region(s). The overall G-value for modelled protein restricta lipase was found to be −0.01, which shows modelled protein is acceptable; a G-value lower than

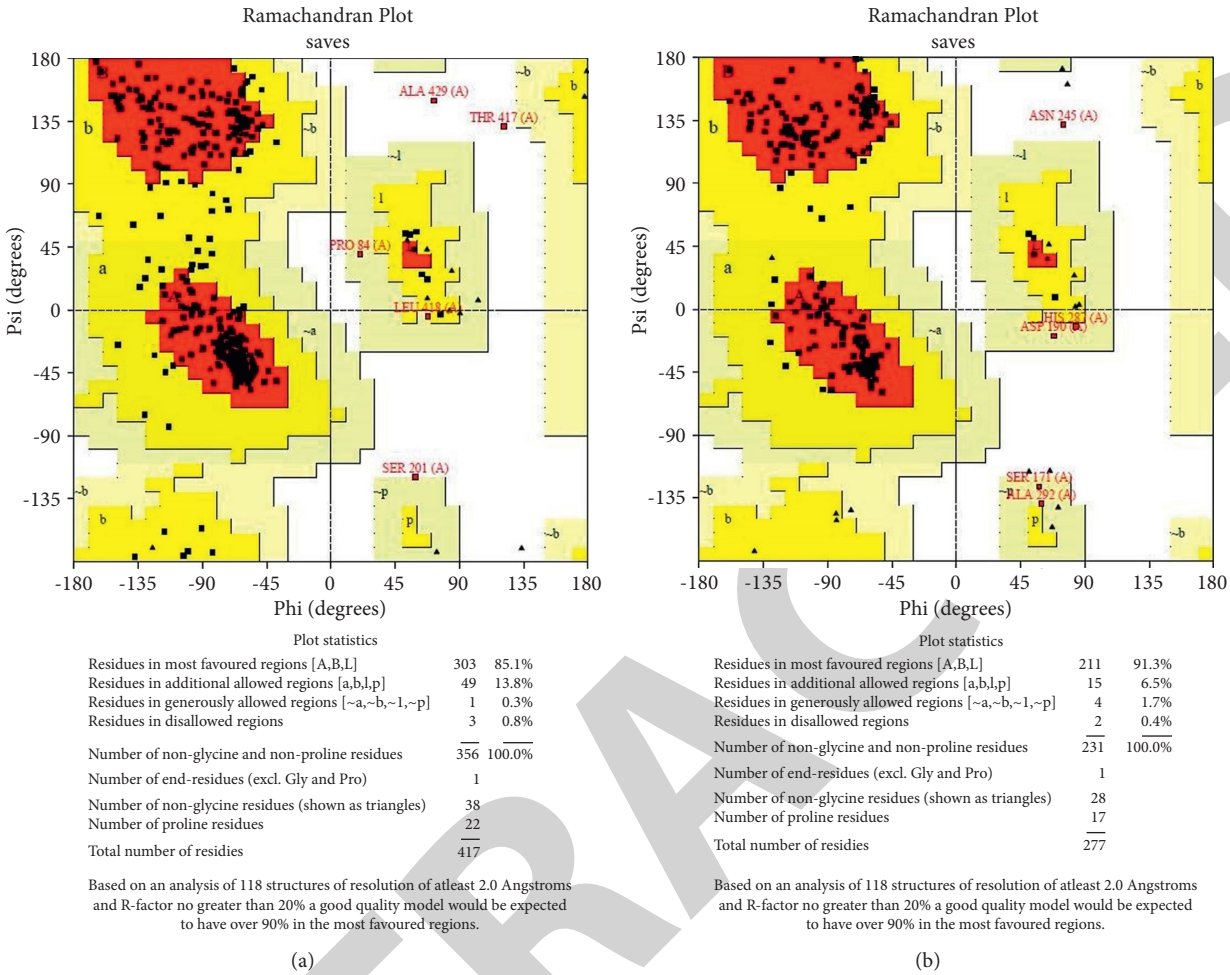

Figure 4: Ramachandran plot for lipase protein of (a) *Malassezia furfur* and (b) *Malassezia restricta*.

−0.5 is considered unusual. The SWISS-MODEL protein models were submitted to the ERRAT server [27, 28], and the model quality factors were found to be 84.804. for furfur lipase and 97.348 for restricta lipase which shows that the built models were error-free and of high quality. The amino acids SER 201, THR 417, and ALA 429 of furfur lipase and ASN 245 of restricta lipase were found to be in the disallowed region of the plot with distorted conformation, which was then submitted to ModLoop and SwissPDB viewer server, and the loops were remodeled and energy minimized, and the conformation was saved in PDB file format to be further used for molecular docking (Figure 5).

3.3. Molecular Docking Studies of Lipase of Malassezia Species. Table 2 depicts the phytocompounds that were subjected to the Lipinski rule of five, which revealed that out of 16 compounds only 11 of them satisfied this rule, and the novel information is that the molecular docking studies of polyherbal extract against the lipase of the Malassezia species were not reported earlier.

3.3.1. Molecular Docking Studies of Lipase Protein from Malassezia globosa. The ligand binding site was predicted with the help of Castp web server, which revealed 17 amino acids: TYR56, GLY100, THR101, ASN102, PHE104, SER105, LEU106, ASN107, HIS170, SER171, LEU172, TRP229, VAL230, ASP278, HIS281, GLN282, ALA292, and VAL293. The molecular docking studies of lipase protein of PDB ID: 4ZRE of *Malassezia globosa* uncloaked that the compound isopropyl stearate showed the least binding energy of −10.107 Kcal/mol, followed by tetradecanoic acid, propyl ester of score −9.805 Kcal/mol, and n-hexadecanoic acid −8.064 Kcal/mol (Table 3). The hydrogen bond is the strongest bond and plays a vital role in supramolecular interactions; thus, the more the number of intermolecular hydrogen bonds, the greater the inhibition efficiency. The isopropyl stearate has formed 2 hydrogen interactions with LEU106 and ASN102 and other interactions like van der Waals interaction with ASN107, GLN278, SER171, HIS170, GLY100, THR101, and GLN282 (Figure 6). The tetradecanoic acid, propyl ester with score of −9.805 Kcal/mol has only formed van der Waals interactions with amino acids residues such as ASP278, VAL230, SER171, GLN278, THR101, ASN102, GLY100, and GLY291, and no conventional hydrogen bond was formed. The n-hexadecanoic acid has formed 3 conventional hydrogen bonds with residues VAL293, MET294, and GLN282. Other interactions were

RETRACTED

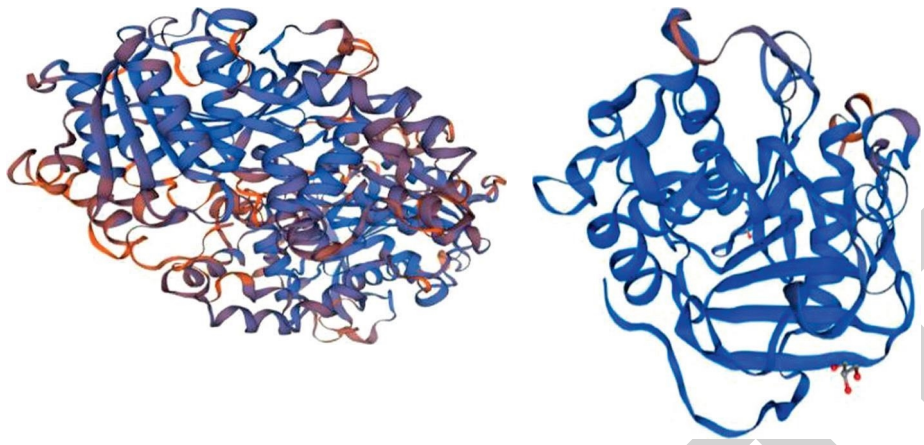

(a) (b)

Figure 5: Lipase protein of (a) *Malassezia furfur* and (b) *Malassezia restricta*.

Table 2: Screening of ligands using Lipinski rule of five.

compound name	Molecular mass (<500 Daltons)	Hydrogen bond donor (<5)	Hydrogen bond acceptor (<10)	Log P (<5)	Molecular refractivity (40–130)
A-pinene	136	0	0	2.998699	43.75798
4-Hydroxy-3-methoxy benzyl alcohol	154	2	3	0.893100	40.581596
Eugenol	164	1	2	2.129300	48.559792
A-caryophyllene	204	0	0	5.035399	68.902977
Humulene-(V1)	204	0	0	4.725199	66.742981
Flavone	222	0	2	3.302799	65.819489
n-Hexadecanoic acid	256	1	2	5.552299	77.947777
Tetradecanoic acid, propyl ester	270	2	5	5.640700	82.327972
Hexadecenoic acid, methyl ester	284	0	2	6.030800	86.944969
8-Octadecenoic acid, methyl ester	296	0	2	6.196900	91.467964
(Z)-13-Octadecenyl acetate	310	0	2	6.587001	96.084961
Phenol,2,4-bis[1,1-dimethylethyl]	282	0	1	6.618799	89.606912
Docosanoic acid, methyl ester	354	0	2	7.981303	110.029953
Trans-A-copaene	204	0	0	4.270899	64.572978
Isopropyl stearate	326	0	2	4.199502	100.773956
2,6-Bis-[3-nitrobenzylidene]-4-methylcyclohexanone	364	0	5	4.722999	101.004768

found such as pi-alkyl, pi-anion interactions van der Waals interactions.

3.3.2. Molecular Docking Studies of Lipase of Malassezia restricta. The molecular docking studies of lipase protein of *Malassezia restricta* reveal that the compounds that showed least binding energies are flavone of score −7.160 Kcal/mol, followed by isopropyl stearate with −6.736 kcal/mol and n-hexadecanoic acid with −6.461 kcal/mol (Table 4). The flavone has formed one conventional hydrogen bond with SER144 and also formed van der Waals interaction with residues such as HIS80, THR104, ILE145, PHE84, MET176, GLY137, and LEU172. The ligand with a greater number of hydrogen bonds shows high binding affinity and effective inhibition against the protein (Figure 7). The isopropyl stearate has a score of −6.736 kcal/mol which has formed other interactions like pi-alkyl, alkyl, and van der Waals interactions with residues THR104, LYS114, GLY137, ASP79, GLU140, HIS80, SER144, GLN82, and PHE84. The n-hexadecanoic acid of score −6.461 kcal/mol has formed one conventional hydrogen bonding with GLN82. The ligand has also van der Waals interactions with residues LEU172, PHE138, GLY137, THR104, MET176, HIS80, SER144, PHE84, and ILE145. The other interactions include pi-sigma, pi-alkyl, and alkyl interactions.

3.3.3. Molecular Docking Studies of Lipase Protein of Malassezia furfur. The molecular docking studies of lipase protein of *Malassezia furfur* uncloak that the compounds that showed least binding energies are eugenol of score −8.296 Kcal/mol followed by A-caryophyllene with −8.131 kcal/mol and trans -A- copaene with −7.641 kcal/mol

RETRACTED

Table 3: Docked conformation of bioactive compounds against the lipase of Malassezia globosa.

compound name	Binding energy (Kcal/mol)	van der Waals interactions	No. of hydrogen bonds	Hydrogen bond residues	Total no. of residues
A-pinene	−4.976	GLY100, THR101, ASN102, HIS281, SER171, ASP278, GLN282, and MET294	0	-	GLY100, THR101, ASN102, HIS281, SER171, ASP278, GLN282, MET294
4-Hydroxy-3-methoxy benzyl alcohol	−6.439	GLY100, GLN282, SER171, HIS281, TYR56, and VAL293	3	THR101 ASN102 ASP278	THR101, ASN102 ASP278, GLY100, GLN282, SER171, HIS281, TYR56, VAL293
Eugenol	−7.073	SER171, ASP278, GLN282, GLY100, TYR56, VAL293, and ASN102	1	THR101	THR101, SER171, ASP278, GLN282, GLY100, TYR56, VAL293, ASN102
A-caryophyllene	−5.308	ASN102, THR101, ASP278, HIS281, GLN282, SER171, and GLY100	0	-	ASN102, THR101, ASP278, HIS281, GLN282, SER171, GLY100
Humulene-(V1)	−5.761	ASP278, GLN282, SER171, GLY100, ASN102, and THR101	0	-	ASP278, GLN282, SER171, GLY100, ASN102, THR101
Flavone	−6.830	ASN102, SER105, LEU172, SER171, HIS281, PHE276, and ASN277	2	ASN107 LEU106	ASN107, LEU106 ASN102, SER105, LEU172, SER171, HIS281, PHE276, ASN277
n-Hexadecanoic acid	−8.064	LEU106, SER171, ASN102, THR101, ASP278, ASN107, and GLY291	3	VAL293 MET294 GLN282	VAL293, MET294 GLN282, LEU106, SER171, ASN102, THR101, ASP278, ASN107, GLY291
Trans-A-copaene	−6.792	ASN102, SER171, HIS170, GLY100, THR101, TYR56, GLN282, MET294, ASP278	0	-	ASN102, SER171, HIS170, GLY100, THR101, TYR56, GLN282, MET294, ASP278
Isopropyl stearate	−10.107	ASN107, GLN278, SER171, HIS170, GLY100, THR101, GLN282	2	LEU106 ASN102	LEU106, ASN102, ASN107, GLN278, SER171, HIS170, GLY100, THR101, GLN282
Tetradecanoic acid, propyl ester	−9.805	ASP278, VAL230, SER171, GLN278, THR101, ASN102, GLY100, GLY291	0	-	ASP278, VAL230, SER171, GLN278, THR101, ASN102, GLY100, GLY291

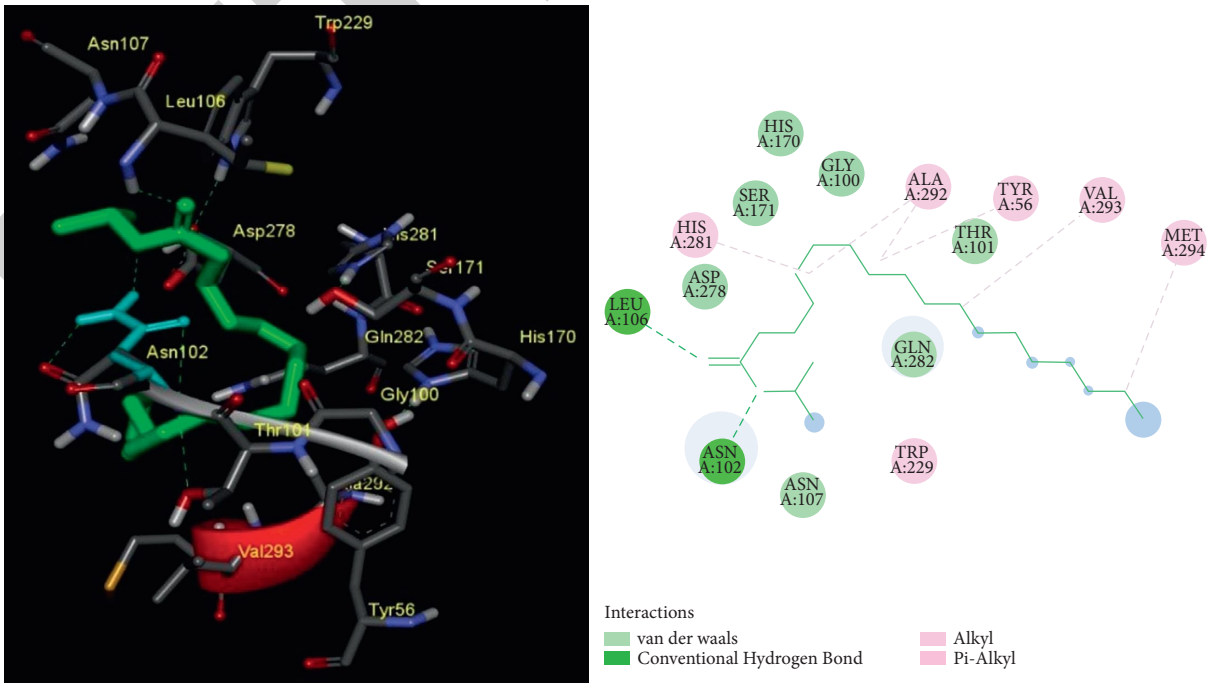

Figure 6: 2D and 3D interaction of Isopropyl stearate of binding score −10.107 Kcal/mol against lipase of *Malassezia globosa*.

RETRACTED

Table 4: Docked conformation of bioactive compounds against the lipase of Malassezia restricta.

compound name	Binding energy (Kcal/mol)	van der Waals interactions	No. of hydrogen bonds	Hydrogen bond residues	Total residues
A-pinene	−4.383	SER144, LYS114, THR104, GLN82, GLY137, GLU140	0	-	SER144, LYS114, THR104, GLN82, GLY137, GLU140
4-Hydroxy 3-methoxy benzyl alcohol	−6.063	THR104, PHE84, GLN82, GLU140	4	GLY137 LYS114 SER144 HIS80	GLY137, LYS114 SER144, HIS80, THR104, PHE84, GLN82, GLU140
Eugenol	−6.186	HIS80, GLN82, SER144, THR104	2	LYS114, GLY137	LYS114, GLY137, HIS80, GLN82, SER144, THR104
A-caryophyllene	−5.610	THR104, GLU140, SER144, HIS80, PHE84, GLN82, LEU172, GLY137	0	-	THR104, GLU140, SER144, HIS80, PHE84, GLN82, LEU172, GLY137
Humulene-(V1)	−5.772	THR104, GLY137, LYS114, GLU140, SER144, HIS80, ARG81, GLN82	0	-	THR104, GLY137, LYS114, GLU140, SER144, HIS80, ARG81, GLN82
Flavone	−7.160	HIS80, THR104, ILE145, PHE84, MET176, GLY137, LEU172	1	SER144	HIS80, THR104, ILE145, PHE84, MET176, GLY137, LEU172, SER144
n-Hexadecanoic acid	−6.461	LEU172, PHE138, GLY137, THR104 MET176, HIS80, SER144, PHE84, ILE145.	1	GLN82	GLN82, LEU172, PHE138, GLY137, THR104, MET176, HIS80, SER144, PHE84, ILE145
Trans-A-copaene	−6.352	GLN82, HIS80, ARG81, GLU140, LYS114, THR104, GLY137, PHE138	0	-	GLN82, HIS80, ARG81, GLU140, LYS114, THR104, GLY137, PHE138
Isopropyl stearate	−6.736	THR104, LYS114, GLY137, ASP79, GLU140, HIS80, SER144, GLN82, PHE84	0	-	THR104, LYS114, GLY137, ASP79, GLU140, HIS80, SER144, GLN82, PHE84
Tetradecanoic acid, propyl ester	−6.287	GLY137, THR104, LYS114, GLN82, HIS80, SER144	0	-	GLY137, THR104, LYS114, GLN82, HIS80, SER144

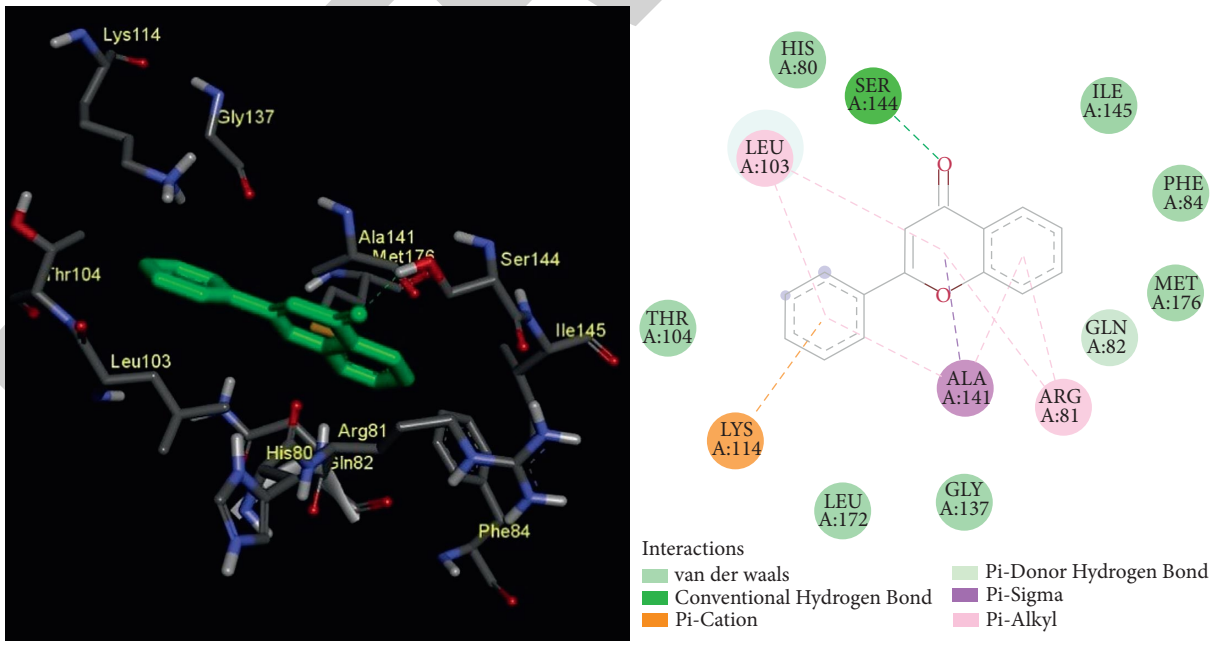

Figure 7: 2D and 3D interactions of flavone of binding score −7.160 Kcal/mol against lipase of *Malassezia restricta*.

(Table 5). The eugenol has formed two conventional hydrogen bonds with ALA111, TYR200 and also formed van der Waals interaction with residues such as LEU137, GLU139, VAL134, PHE135, PHE141, GLY199, TYR198, SER109, GLY203, and SER201. The ligand with a greater number of hydrogen bonds shows high binding affinity and effective inhibition against the protein (Figure 8). The A-caryophyllene has a score of −8.131 kcal/mol, which has

Table 5: Docked conformation of bioactive compounds against lipase of Malassezia furfur.

compound name	Binding energy (Kcal/mol)	van der Waals interaction	No. of hydrogen bonds	Hydrogen bond residues	Total residues
A-pinene	−5.945	ASP138, TYR200, GLY199, SER109, and GLY108	0	-	ASP138, TYR200, GLY199, SER109, and GLY108
4-Hydroxy 3-methoxy benzyl alcohol	−7.521	PHE62, TYR125, PHE135, GLU139, PHE142, PHE141, GLY199, TYR198, and GLY203	4	VAL134 ALA111 SER109 TYR200	VAL134, ALA111 SER109, TYR200, PHE62, TYR125, PHE135, GLU139, PHE142, PHE141, GLY199, TYR198, and GLY203
Eugenol	−8.296	LEU137, GLU139, VAL134, PHE135, PHE141, GLY199, TYR198, SER109, GLY203, and SER201	2	ALA111 TYR200	LEU137, GLU139, VAL134, PHE135, PHE141, GLY199, TYR198, SER109, GLY203, SER201, ALA111, and TYR200
A-caryophyllene	−8.131	PHE62, GLU139, PHE135, ASP138, TYR125, VAL134, PHE141, GLY108, SER109, GLY199, GLY203, TYR200, and GLY386	0	-	PHE62, GLU139, PHE135, ASP138, TYR125, VAL134, PHE141, GLY108, SER109, GLY199, GLY203, TYR200, and GLY386
Humulene-V1	−7.501	SER109, GLU386, GLY203, VAL134, TYR125, GLU139, GLY199, and ASP138	0	-	SER109, GLU386, GLY203, VAL134, TYR125, GLU139, GLY199, and ASP138
Flavone	−5.875	TYR198, GLY199, TYR200, SER201, VAL110, VAL134, PHE135, GLU139, PHE62, and PHE141	0	-	TYR198, GLY199, TYR200, SER201, VAL110, VAL134, PHE135, GLU139, PHE62, and PHE141
n-Hexadecanoic acid	−5.824	TYR145, TYR125, PHE135, PHE62, GLU139, LEU137, ASP138, GLY203, GLY199, TYR200, and GLU386	1	SER109	SER109, TYR145, TYR125, PHE135, PHE62, GLU139, LEU137, ASP138, GLY203, GLY199, TYR200, and GLU386
Trans-A-copaene	−7.641	GLU386, TYR200, TYR198, GLY199, SER109, ALA111, ASP138, GLU139, VAL134, and PHE62	0	-	GLU386, TYR200, TYR198, GLY199, SER109, ALA111, ASP138, GLU139, VAL134, and PHE62
Isopropyl stearate	−2.321	SER201, GLY203, GLY199, GLY108, SER109, TYR125, PHE135, ASP138, GLU386, GLU139, and PHE62	0	-	SER201, GLY203, GLY199, GLY108, SER109, TYR125, PHE135, ASP138, GLU386, GLU139, and PHE62
Tetradecanoic acid, propyl ester	−1.483	GLY203, GLY199, GLY108, PHE141, VAL134, LEU137, PHE135, GLU139, ASP138, PHE62, TYR125, SER201, and GLU386	1	TYR200	TYR200, GLY203, GLY199, GLY108, PHE141, VAL134, LEU137, PHE135, GLU139, ASP138, PHE62, TYR125, SER201, and GLU386

formed other interactions like pi-alkyl, alkyl, and van der Waals interactions. The A-caryophyllene has no conventional hydrogen bonding. The Trans-A-copaene of score −7.641 kcal/mol has not formed any conventional hydrogen bonding with the protein but has formed van der Waals interactions with residues GLU386, TYR200, TYR198, GLY199, SER109, ALA111, ASP138, GLU139, VAL134, and PHE62. The other interactions include pi-sigma, pi-alkyl, and alkyl interactions.

3.3.4. Screening of Drug Properties. The drug properties (Supplementary Information) viz., absorption, distribution, metabolism, and excretion properties of the top five compounds with the best binding energies against the three proteins were reported. All the compounds showed very good gastrointestinal absorption properties above 80%. None of the compounds were P-glycoprotein substrate except A-caryophyllene and flavone and inhibitors. The compounds also showed satisfactory blood-brain barrier and central nervous system permeability properties. The compounds were neither CYP2D6 substrate nor CYP2C9, CYP2D6, and CYP3A4 inhibitors. Compounds such as flavone, n-hexadecanoic acid, Trans-A-copaene, isopropyl stearate and tetradecanoic acid, and propyl ester were CYP3A4 substrates. The compounds flavone, Trans-A-copaene, isopropyl stearate and tetradecanoic acid, and propyl ester were CYP1A2 inhibitors, and flavone was the inhibitor of CYP2CI9. None of the compounds reported AMES mutagenic property except eugenol and flavone. No compounds were hERG I inhibitor. The compounds were safe and were not hepatotoxic in nature. All compounds

RETRACTED

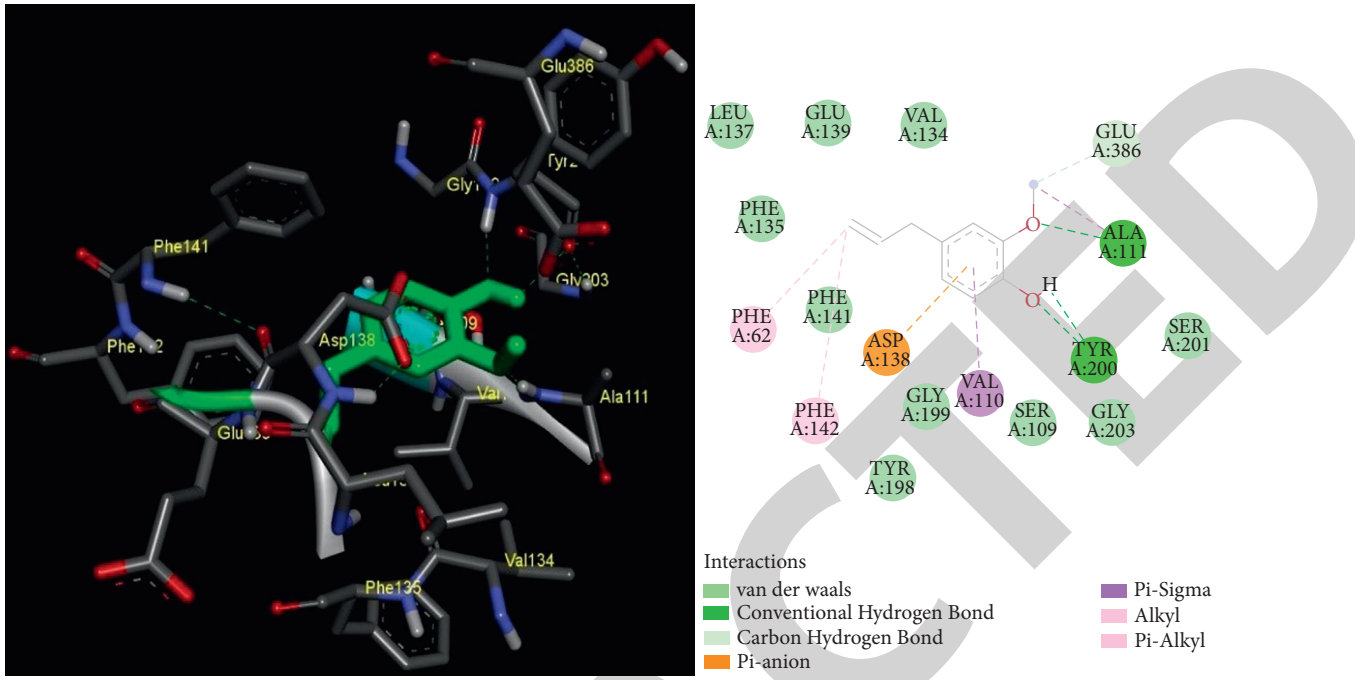

Figure 8: 2D and 3D interactions of eugenol of binding score −8.296 Kcal/mol against lipase of *Malassezia furfur*.

reported skin sensitisation property except A-pinene, 4-hydroxy-3-methoxy benzyl alcohol, flavone, and Trans-A-copaene.

4. Conclusion

Thus, the polyherbal ethanolic extract containing the components of *Murraya koenigii*, *Moringa oleifera,* and *Psidium guajava* reveals that the antidandruff property of the extract studied with the molecular docking has enhanced in an optimistic manner, where the 11 phytocompounds that satisfied the Lipinski rule have shown exceptional binding scores against the lipase. None of the compounds were reported as the carcinogen, cardiotoxic, and hepatotoxic. Therefore, the compounds were safe for consumptions. Hence, the lipase which is responsible for the growth and pathogenicity of the *Malassezia* species can be inhibited effectively by the polyherbal ethanolic extract. Further, these polyherbs can be used for hair care product preparation for its antidandruff property, which can be validated by In-vitro and In-vivo studies.

Data Availability

The data used to support the findings of the study can be obtained from the corresponding author upon request.

Conflicts of Interest

The authors declare that they have no conflicts of interest.

Supplementary Materials

The supplementary material contains 4 tables (Tables 6–9). Table 6 gives the information about absorption properties of the polyherbal extract. Table 7 conveys the distribution property details of the polyherbal extract. Table 8 gives the information about the metabolism properties of the polyherbal extract. Table 9 conveys about the excretion and toxicity property of polyherbal extract. This information is discussed in Section 3.3.4, Screening of Drug Properties. (*Supplementary Materials*)

References

[1] M. Narshana and P. Ravikumar, "An overview of dandruff and novel formulations as atreatment strategy," *IJPSR*, vol. 9, no. 2, pp. 417–431, 2018.

[2] S. M. Rudramurthy, P. Honnavar, S. Dogra, P. P. Yegneswaran, S. Handa, and A. Chakrabarti, "Association of Malassezia species with dandruff," *The Indian journal of medical research*, vol. 139, no. 3, pp. 431–7, 2014.

[3] Z. Xu, Z. Wang, C. Yuan et al., "Dandruff is associated with the conjoined interactions between host and microorganisms," *Scientific Reports*, vol. 65 pages, 2016.

[4] C. Clavaud, R. Jourdain, A. Bar-Hen et al., "Dandruff is associated with disequilibrium in the proportion of the major bacterial and fungal populations colonizing the scalp," *PLoS One*, vol. 8, no. 3, Article ID e58203, 2013.

[5] M. Shivaprakash, P. Honnavar, S. Dogra, P. Prakash, H. Sanjeev, and C. Arunaloke, "Association of Malassezia species with dandruff," *Indian Journal of Med Research*, vol. 139, no. 3, pp. 431–437, 2014.

[6] T. O. WeerapongJuntachai, S. Y. Murayama, and S. Kajiwara, "The lipolytic enzymes activities of Malassezia species," *Medical Mycology*, vol. 47, no. 5, pp. 477–484, 2009.

[7] W. Juntachai, T. Oura, S. Y. Murayama, and S. Kajiwara, "The lipolytic enzymes activities of *Malassezia* species," *Medical Mycology*, vol. 47, no. 5, pp. 477–484, 2009.

[8] M. koenigii, *Curry Leaf Tree*, CABI, Wallingford, UK, 2018.

RETRACTED

[9] M. S. koenigii, C. Parmar, and M. K. Kaushal, *Wild Fruits*, pp. 45–48, Kalyani Publishers, New Delhi, India, 1982.
[10] P. Gupta and D. Nahata, "An update on Murrayakoenigii S: a multifunctional ayurvedic herb," *Journal of Chinese Integrative Medicine*, vol. 9, no. 8, pp. 824–833, 2012.
[11] S. C. Saini and Reddy, "A review on curry leaves (Murrayakoenigii): versatile multi-potential medicinal plant," *American Journal of Phytomedicine and Clinical Therapeutics AJPCT*, vol. 3, no. 4, pp. 363–368, 2015.
[12] M. koenigii, *Curry Leaf Tree (Murrayakoenigii*, Heritage Garden, Chennai, Tamil Nadu, 2019.
[13] L. Gopalakrishnan and K. Doriya, D. S. Kumar and M. Oleifera, A review on nutritive importance and its medicinal application," *Food Science and Human Wellness*, vol. 5, no. 2, pp. 49–56, 2016.
[14] F. Farooq, M. Rai, A. Tiwari, A. A. Khan, and S. Farooq, "Medicinal properties of Moringa oleifera: an overview of promising healer," *Journal of Medicinal Plants Research*, vol. 6, no. 27, pp. 4368–4374, 2012.
[15] S. Naseer, S. Hussain, N. Naeem, and Pervaiz, "The phytochemistry and medicinal value of *Psidium guajava* (guava)," *Clin Phytosci*, vol. 432 pages, 2018.
[16] G. Studer, C. Rempfer, A. M. Waterhouse, R. Gumienny, J. Haas, and T. Schwede, "QMEANDisCo—distance constraints applied on model quality estimation," *Bioinformatics*, vol. 36, no. 6, pp. 1765–1771, 2020.
[17] R. A. Laskowski, J. A. Rullmann, M. W. MacArthur, R. Kaptein, and J. M. Thornton, "AQUA and PROCHECK-NMR: programs for checking the quality of protein structures solved by NMR," *Journal of Biomolecular NMR*, vol. 8, no. 4, pp. 477–486, 1996.
[18] F. Sievers, A. Wilm, D. Dineen et al., "Fast, scalable generation of high-quality protein multiple sequence alignments using Clustal Omega," *Molecular Systems Biology*, vol. 7, no. 1, 539 pages, 2011.
[19] D. J. Pagliarini, S. E. Wiley, M. E. Kimple et al., "Involvement of a mitochondrial phosphatase in the regulation of ATP production and insulin secretion in pancreatic β cells," *Molecular Cell*, vol. 19, no. 2, pp. 197–207, 2005.
[20] N. Riaz, P. Blecua, R. S. Lim et al., "Pan-cancer analysis of bi-allelic alterations in homologous recombination DNA repair genes," *Nature Communications*, vol. 8, no. 1, pp. 1–7, 2017.
[21] T. Schwede, J. Kopp, N. Guex, and M. C. Peitsch, "SWISS-MODEL: an automated protein homology-modeling server," *Nucleic Acids Research*, vol. 31, no. 13, pp. 3381–3385, 2003.
[22] V. Harini, M. Vijayalakshmi, C. Sivaraj, and P. Arumugam, "Antioxidant and anticancer activities of methanol extract of *melochiacorchorifolia* L," *International Journal of Scientific Research*, vol. 6, no. 1, pp. 1310–1316, 2017.
[23] R. Abhishek Biswal, A. Aishwarya, A. Sharma, and P. Vivek, "2D QSARadmet prediction and multiple receptor molecular docking strategy in bioactive compounds of Gracilariacorticata against Plasmodium falciparum (contractile Protein)," *Informatics in Medicine Unlocked*, vol. 17, Article ID 100258, 2019.
[24] R. Abhishek Biswal, V. Pazhamalai, A structure based molecular docking of Acacia catechu against contractile protein Plasmodium falciparum –amalarial disease," *International Journal of Pharm. Science Drug Res. November-December*, vol. 12, no. 1, 2020.
[25] G. N. Nirmala, A. Sharma, D.K. Dharani, and R. Venkatraghavan, "Effect of essential oil of Santalum album against covid-19, lung cancer and streptococcal pneumonia: an Insilco approach," *Solid State Technology*, vol. 63, no. 6, 2020.
[26] R. Abhishek Biswal, s. Akshata, A. Aishwarya, and V. Pazhamalai, "Molecular docking and admet studies of bioactive compounds of *rhizoporamucornata* against bacterial eenzymeprotein tyrosine phosphatase," *IJPSR*, vol. 11, no. 4, 2020.
[27] G. N. Ramachandran, C. Ramakrishnan, and V. Sasisekharan, "Stereochemistry of polypeptide chain configurations," *Journal of Molecular Biology*, vol. 7, no. 1, pp. 95–99, 1963.
[28] C. Colovos and T. O. Yeates, "Verification of protein structures: patterns of nonbonded atomic interactions," *Protein Science*, vol. 2, no. 9, pp. 1511–1519, 1993.

RETRACTED